Article

Optimal SOFC-CHP Installation Planning and Operation Model Considering Geographic Characteristics of Energy Supply Infrastructure

Takashi Owaku [1] , Hiromi Yamamoto [1,2] and Atsushi Akisawa [3,*]

[1] Graduate School of Bio-Applications and Systems Engineering, Tokyo University of Agriculture and Technology, Koganei 184-8588, Japan

[2] Grid Innovation Research Laboratory, Central Research Institute of Electric Power Industry, Yokosuka 240-0196, Japan

[3] Institute of Engineering, Tokyo University of Agriculture and Technology, Koganei 184-8588, Japan

* Correspondence: akisawa@cc.tuat.ac.jp

Abstract: Combined heat and power (CHP) is crucial for promoting thorough energy conservation and advanced energy use, aimed toward greenhouse gas reduction. Solid oxide fuel cell (SOFC)-CHP is expected to be introduced as a measure against global warming and has been the focus of attention, and this study examined the effects of its introduction. This study introduces a linear programming evaluation model that can simulate optimized facility configuration and operation, based on the power supply and demand. The novelty of the proposed model is the consideration of geographic characteristics, which influences parameters dependent on gas transportation infrastructure and electricity. A sensitivity analysis was conducted considering the number of units and location of SOFC-CHP introductions in the National Capital Region of Japan. As a result, it was predicted that SOFC-CHP would likely begin to be introduced in areas where there is a large shadow price difference between electricity and gas at each node. The total power generation will decrease, as transmission and distribution losses decrease, owing to the diffusion of SOFC-CHP installed in the vicinity of demand. The widespread use of SOFC-CHP is an economically feasible CO_2 emissions reduction pathway. These results will help assess the introduction of various distributed power sources in addition to SOFC-CHP to reduce CO_2 emissions.

1. Introduction

1.1. Motivation

On November 2021, the 26th United Nations Climate Change Conference of the Parties agreed to pursue efforts to limit the temperature increase to 1.5 °C above pre-industrial levels [1]. The Paris Agreement established goals to respond to and mitigate the frequent occurrence of abnormal weather events, such as heavy rains and heat waves, around the world caused by global warming. Over 120 countries and regions, including Japan, have pledged to achieve carbon neutrality by 2050. In light of these circumstances, a new Strategic Energy Plan [2], which governs the fundamental direction of Japan's energy policy, was approved by the Cabinet in October 2021. An important theme of this plan is the achievement of carbon neutrality by 2050. It includes a roadmap for Japan's energy policy toward an intermediate goal of 46% reduction in greenhouse gas emissions by 2030. The key policy agenda for the 2030 goal is to encourage the maximum introduction of renewable energy sources, based on the premise of safety, to realize a stable energy supply at low cost through improved economic efficiency, while simultaneously ensuring environmental compatibility.

To this end, heat demand, which accounts for approximately 60% of the energy consumption of Japan's consumer and industrial sectors [2], can be considered an area of focus. As these energy demands are indispensable to people's livelihood, the decarbonization of heat demand is crucial for achieving carbon neutrality by 2050. Another policy agenda for the 2030 intermediate goal is to encourage the introduction and expansion of non-fossil energy through demand-side electrification and promoting thorough energy conservation and advanced use of energy. In this respect, the combined heat and power (CHP) approach shows considerable promise [3]: the CHP approach has been emphasized for its advantages by the United States Department of Energy toward the Combined Heat and Power Deployment Program [4]; furthermore, nine European manufacturing organizations have requested to the European Union to encourage the use of high-efficiency CHP [5].

1.2. Literature Survey

In a previous study, Li et al. [6] proposed a hybrid concentrating solar power (CSP)-CHP system that provides power system operational flexibility for renewable energy deployment; the CSP-CHP system was shown to be effective in promoting renewable energy. Ahn et al. [7] suggested that CHP systems could support grid flexibility to address generation uncertainty and variability arising because of the increased use of renewable energy; they indicated that the use of available CHP can discourage the installation of new power plants. Narayanan et al. [8] conducted energy simulations in a distributed residential energy system comprising a solar thermal collector, photovoltaic power generation (PV), lithium-ion batteries, and a solid oxide fuel cell (SOFC) CHP for natural gas, and observed that the SOFC-CHP system allowed 100% self-sufficiency with respect to electricity demand and that the self-sufficiency ratio of the distribution system can be improved by 10%. Similarly, previous studies have been conducted on the energy conservation in addition to the CO_2 reduction effects of introducing SOFC-CHP in the residential sector. Arinami et al. [9], Yuasa et al. [10], and Aoki et al. [11] showed that installing an appropriate capacity of fuel cell CHP can save more than 10% energy compared to conventional facilities and an emission reduction of approximately 3.0 t-CO_2/year per household. Nielsen et al. [12] demonstrated that 1000 units of SOFC-CHP can reduce CO_2 emissions by over 10%. Similar studies on SOFC-CHP installations in the commercial sector have also been conducted. Palomba et al. [13] experimented and numerically analyzed a small-scale multiple power generation system combining SOFC-CHP and a thermally driven adsorption chiller and reported energy savings of up to 110 MWh/year and CO_2 emission reductions of 43 t-CO_2/y. Jing et al. [14] showed that carbon emission reductions of up to 61% per year could be achieved by installing the appropriate SOFC-CHP and absorption chiller capacities for hospitals. Alns and Sleiti [15] studied commercial buildings and showed that installing a combined SOFC-CHP and electric absorption chiller system can improve the overall energy efficiency of a building and can reduce CO_2 emissions by 30%. Although these studies have been conducted on the energy-saving and CO_2 reduction effects of SOFC-CHP systems, they do not consider the geographical characteristics of the energy system and are limited to cities and buildings of a certain size; moreover, they focus only on operational analysis. It is important to consider regional characteristics and energy transportation when optimizing energy systems from a macro perspective.

Oshiro and Masui [16] incorporated and evaluated CHP through energy supply and demand in greenhouse gas emission reductions in Japan using a detailed sector-split model for Japan. Nagata et al. [17] performed a case study using the World Energy System (Dynamic New Earth 21+) to evaluate CHP while considering the analysis of the significance of fuel conversion to natural gas in the mid- to long-term global warming strategy. However, these studies did not consider in detail the transmission of electricity or the transport of gas within the region. Sugiyama et al. [18] considered electricity distribution and analyzed the mass deployment of variable renewable energy sources such as PV and wind power using an optimal generation mix model that considered the detailed high-voltage power grid throughout Japan; however, this study did not consider gas transportation.

Johanna et al. [19] evaluated the cost competitiveness of CHP plants by comparing multiple energy system levels (regional, urban, and plant) and confirmed the effects of electricity and biomass prices; however, their model does not consider the effects of electricity and gas supply infrastructure.

The benefits and potential of fuel cells and other distributed power sources are being studied for supporting power grid operations. Most previous studies [20–24] showed that it is possible to increase power quality, improve reliability and resiliency, and provide ancillary services in situations where large amounts of distributed renewable energy resources are deployed. Prior studies [25,26] have demonstrated the potential of fuel cell CHP and other sources to support grids with high renewable energy deployment in the future. As these studies were focused on grid operation, the economy of the installation of distributed power supplies have not been considered in the planning, construction, and operation of power supply facilities.

To summarize this section, previous studies [7–15] that considered electricity and heat demands have been conducted only in small-scale areas. On the other hand, most of the previous studies [16–19] that considered large-scale areas treated only electricity demand, and only a few studies considered energy supply infrastructure. In addition, previous studies [20–26] that considered the placement of distributed power sources often did not consider installation planning and operation. Based on the above, few studies have been conducted using facility installation planning and operation models that simultaneously consider electricity and heat demand as well as the geographic characteristics of the energy supply infrastructure.

1.3. Contributions

The present study is unique in that it uses a model that can simulate optimal facility configuration and operation, considering not only the geographical characteristics of electricity and gas systems, but also energy transport within the region. This study will make it possible to reduce transmission losses by introducing distributed power sources such as CHP, reducing congestion in electricity and gas transportation, and planning the optimization of the entire energy system based on local demand and renewable energy characteristics, taking into account the energy transportation infrastructure as well. The results of this study are expected to provide useful knowledge for considering future strategies for the introduction of distributed generation. Furthermore, unlike the existing literature, which focuses on gas engine CHP, this study focuses on SOFC-CHP. SOFC is strongly desired for commercialization in the future for the following reasons: it has a high-power generation efficiency; it is compatible with a variety of fuels, such as natural gas and coal gas; it is widely adaptable from small distributed systems to large-scale alternative thermal power systems; and it is expected to become increasingly widespread after 2025 [27]. The sensitivity analysis of SOFC-CHP using the model constructed in this study will facilitate the quantification of target costs for SOFC-CHP diffusion, which approximately reflects actual conditions, and the use of this model can clearly demonstrate the selection of optimal installation areas based on the usage of electricity and gas supply infrastructure. In addition, because it is possible to account for the transmission losses reduced by SOFC-CHP installed near consumers, it is also possible to specify the effect of reduced total power generation and CO_2 emissions owing to the introduction of SOFC-CHP. The methodology used in this study is expected to contribute to the study of the target cost and the optimization of distributed generation deployment specific to each country.

1.4. Paper Organization

The rest of this paper is organized as follows: Section 2 outlines the optimal facility configuration and operation simulation model for the supply and demand, which considers geographical characteristics as well as heat demand, and presents the data used in the simulation. Section 3 discusses the results of sensitivity analysis, the impact of geographical

characteristics of the installation, and the CO_2 reduction effect of SOFC-CHP installation. Section 4 summarizes the primary conclusions.

2. Materials and Methods

2.1. Data

The proposed evaluation model comprised three major components: a power grid sub-model, city gas grid sub-model, and consumer facilities sub-model, each of which is coupled by the supply and demand of electricity and city gas. A conceptual diagram of the model is shown in Figure 1. To account for geographical characteristics, including the influence of transportation infrastructure, the model divides the target region into smaller regions. However, the larger the target region, the larger the number of areas to be divided, rendering it impossible to solve the problem in a realistic amount of time. Therefore, instead of the entirety of Japan, Japan's National Capital Region was selected as the target region in this model. The National Capital Region comprises the capital city of Tokyo and seven prefectures and is the political and economic center of Japan. Figure 2 shows the location of the National Capital Region. The National Capital Region is characterized by the concentration of one-third of Japan's total population and the enormity of the economic zone, contributing to approximately 1 trillion USD of the gross domestic product of the country as of 2017. In this model, the National Capital Region was divided into 26 demand nodes. Each region's demand is treated as being concentrated at one specific point within the region.
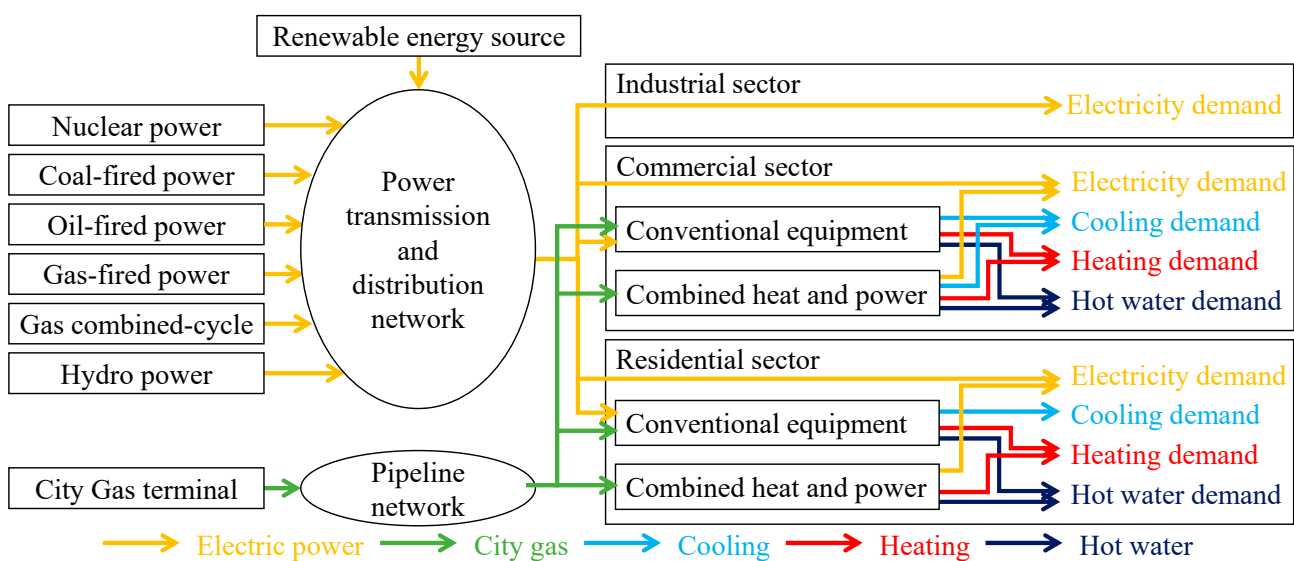

Figure 1. Conceptual schematic of the evaluation model.

2.2. Methods for the Model Development

The model is based on a unified consideration of the power grid sub-model, city gas grid sub-model, and consumer facilities sub-model, which enable optimization based on their interaction with each other. The model is expressed as a linear programming problem with the objective function of minimizing the total annual system cost as shown in Equation (1):

$$minimize\ TC = EFIX + TFIX + GFIX + DFIX + EFUEL + GFUEL \tag{1}$$

Figure 2. Location of the National Capital Region in Japan.

2.2.1. Power Grid Sub-Model

A unique feature of the power grid model is that grid power sources are additionally tagged with corresponding geographic locations; furthermore, transmission lines were considered. Seven types of grid power sources were assumed: nuclear, oil-fired, gas-fired, gas turbine combined cycle power (GTCC), coal-fired, general hydropower, and pumped storage hydropower. The lower capacity limit for each power source was set to the target capacity for 2030 [28], and only GTCC was introduced as a new grid power source. Additionally, generation facilities on the consumer side were considered as reserve margin, and constraints were set as shown in Equation (2):

$$\sum_i \sum_j (1 - loss)(1 - shonai_i) \cdot zg_{j,t} \cdot Yall_{i,j} + \sum_l \sum_p \left(SOFC_{l,p} + SGEN_{l,p} \right) \geq (1 + ze) \sum_l \frac{De_{l,s,t}}{1 - dloss} \quad (2)$$

Because of its large uncertainty in output fluctuation, PV was excluded from the reserve margin. The electric power transport infrastructure comprising the transmission and substation facilities were considered to contain 53 high-voltage lines of 500 kV and 275 kV, and a high-voltage substation that connects them to the lower system. The capacities and locations of existing power sources and transmission line routes are shown in Figure 3. For convenience of incorporation into the linear programming model, the transmission losses in the load flow calculation were exogenously set to a loss rate that is consistent with reality and expressed as shown in Equation (3). The matrices AF and AD used in Equation (3) represent the load flow calculations calculated from the existing transmission line capacity:

$$F_{k,s,t} = \sum_i AF_{k,i} \left\{ (1 - loss) \cdot X_{i,j,s,t} - \frac{St_{i,s,t}}{1 - loss} \right\} - \sum_l AD_{k,l} \cdot \frac{De_{l,s,t}}{1 - dloss} \quad (3)$$
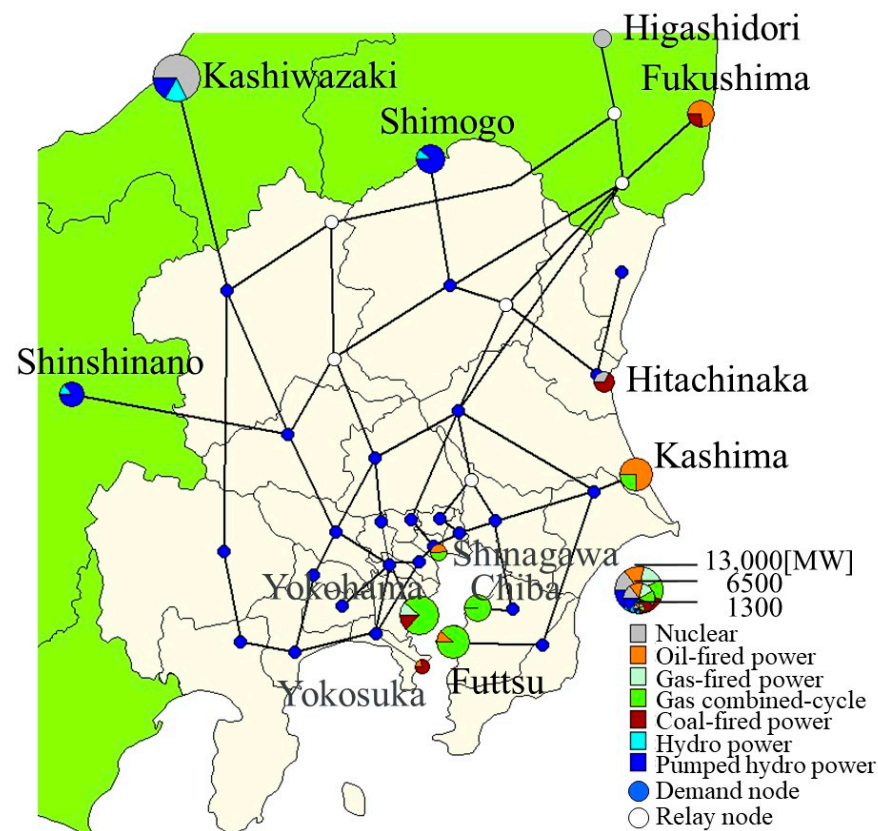
Figure 3. Power network map.

For transmission line reinforcement, only the routes of existing transmission lines were allowed to be reinforced. The various parameters of the power grid model, set up with reference to the literature [29], are shown in Tables 1 and 2.

Table 1. Exogenous variables of power plants.

Type		Nuclear	Coal	Oil	Gas	GTCC [1]	Hydro	Pumped
Unit construction cost [USD/kW]		3180	2470	2610	1890	1490	3640	2180
Lifetime [year]		40	40	60	40	40	60	60
Annual O&M [2] cost rate [%]		4.0	4.8	3.9	3.6	3.6	2.0	1.0
Own consumption rate [%]		4.0	6.0	5.0	4.0	2.0	0.5	0.5
Efficiency [%]		100	42	39	40	57	100	65
CO_2 emission intensity [kg-CO_2/kWh]		0	0.8	0.61	0.45	0.31	0	0
Maximum increase rate of output [%/hour]		0	26	44	44	44	100	100
Maximum decrease rate of output [%/hour]		0	31	31	31	31	100	100
Availability [%]	Seasonal peak	100	85.7	90.1	91.6	93.1	85	85
	Summer (weekday)	93.7	79	87.1	89.1	87.2	85	85
	Summer (holiday)	94.9	80	87.6	89.3	88.4	85	85
	Winter (weekday)	93.2	84.5	78.2	80.3	80.9	62	62
	Winter (holiday)	91.6	85.7	79.1	81.3	79.6	62	62
	Middle (weekday)	83.3	63.3	71.5	71.3	81.1	84	84
	Middle (holiday)	82.5	61.9	71.4	70.4	81.7	84	84
Existing capacity in 2030 [MW]		10,697	5700	10,050	1000	19,129	3009	10,396

[1] GTCC—gas turbine combined cycle power. [2] O&M—operation and maintenance.

Table 2. Exogenous variables of transmission line and substation.

Type	Transmission Line		Substation
	Overhead	Underground	
Unit construction cost	1.55 [USD/kVA/km]	9.09 [USD/kVA/km]	145 [USD/kVA]
Lifetime [year]	50	50	50

2.2.2. City Gas Grid Sub-Model

Similar to the power grid model, geographical characteristics were considered for the city gas grid. With reference to the Japan Gas Association's gas business handbook [30], a lower capacity limit for city gas terminal was set, and 34 high-pressure pipelines were considered to connect the regions. The supply–demand balance of city gas was set based on Equation (4). The matrices AG and AP used in Equation (4) represent the connection relationships between demand nodes and pipelines.

$$Dg_{l,s,t} = \sum_n AP_{n,l} \cdot PF_{n,s,t} + \sum_m AG_{m,l} \cdot Make_{m,s,t} \tag{4}$$

The location of the existing city gas terminal and the pipeline route are shown in Figure 4. As with the transmission line expansion, the pipeline can only be expanded along the existing route. Table 3 shows the parameters set in the city gas supply model with reference to the literature [31,32].
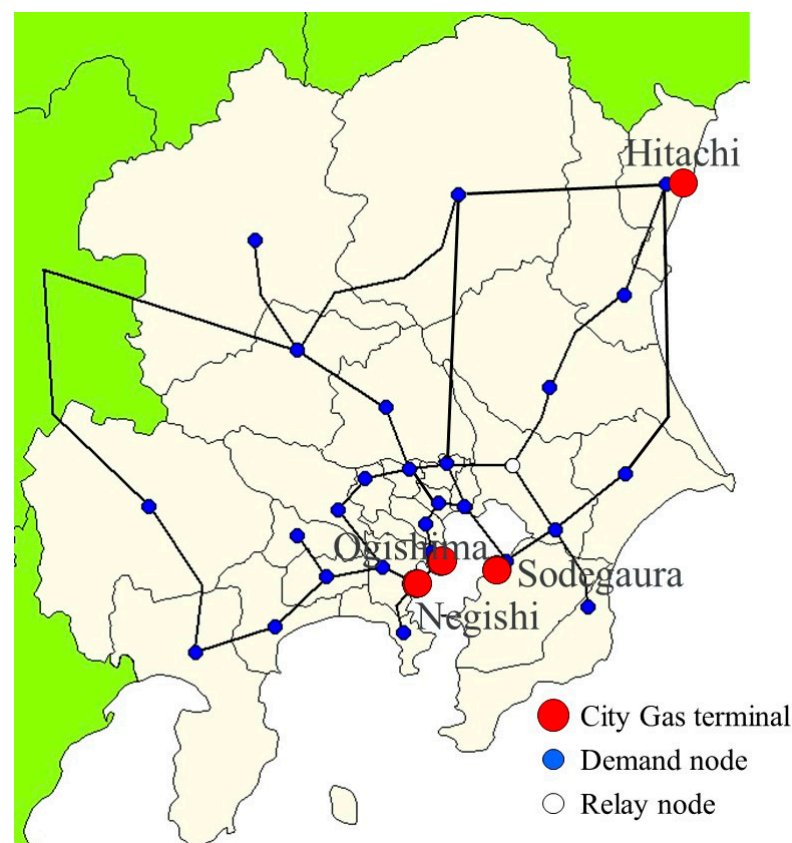

Figure 4. Gas network map of the National Capital Region in Japan.

Table 3. Exogenous variables of gas network.

Type	City Gas Terminal	Pipeline
Unit construction cost	140 [USD/kW]	2.91 [USD/kW/km]
Lifetime [year]	50	50
Annual O&M cost rate [%]	4	4
City gas production cost [USD/kWh]	0.05	
CO_2 emission intensity [kg-CO_2/kWh]	0.18	

2.2.3. Consumer Facilities Sub-Model

The consumer facilities sub-models are classified into three categories: residential, commercial, and industrial. For residential and commercial, electricity and heat demand were set by multiplying the load pattern per unit floor area by the floor area of each demand node, with reference to the literature [33–39]. These two sectors were targeted for the introduction of SOFC-CHP, and the number of installations and extent of operation were optimized using the model. In general, SOFCs cannot be started and shut down frequently, because they are operated at temperatures higher than 700 °C. Therefore, as shown in Equations (5) and (6), the system was set to operate continuously at a minimum load factor of 50% or more:

$$SOFCop_{l,p,s,t} \geq minLF \cdot SOFC_{i,p} \tag{5}$$

$$SGENop_{l,p,s,t} \geq minLF \cdot SGEN_{i,p} \tag{6}$$

Energy flow patterns for the residential and commercial sectors are shown in Figure 5. The commercial sector was further classified into four categories with large market shares: hotels, hospitals, offices, and stores. In addition, as there are some commercial spaces, such as offices and stores, exhibiting small heat demand, SOFC as a generator that does not use waste heat (known as SGEN) was considered as one of the consumer devices. The parameters of the considered consumer equipment were selected based on the study by Sumitomo et al. [40] and are shown in Tables 4–7.
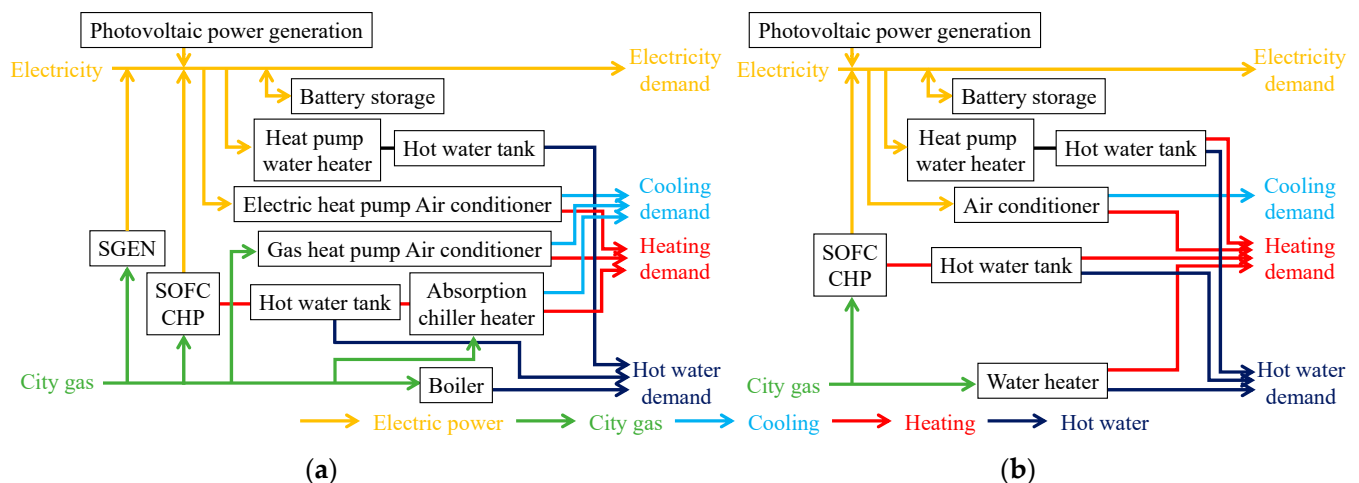

Figure 5. Energy flow of each (**a**) commercial and (**b**) residential consumer. CHP—combined heat and power; SOFC—solid oxide fuel cell; SGEN—SOFC generator that does not use waste heat.

Table 4. Exogenous variables of solid oxide fuel cell.

Type	Commercial (SOFC)	Commercial (SGEN)	Residential (SOFC)
Unit construction cost [USD/kW]	4550	4550	6450
Lifetime [year]	15	15	15
Hot water storage tank [L/kW]	40		20
Stored hot water temperature [°C]	60		70
Power generation efficiency [%]	49.5	53	46.8
Exhaust heat recover efficiency [%]	27		31.5
Minimum load factor [%]	50	50	50

Table 5. Exogenous variables of commercial equipment.

Type	Electric Heat Pump Air Conditioner	Gas Heat Pump Air Conditioner	Absorption Chiller Heater	Heat Pump Water Heater	Boiler
Unit construction cost [USD/kW]	470	1340	235	1270	73.6
Lifetime [year]	15	15	15	15	15
Efficiency (heating)	4.2	1.45	0.87	3.1	0.86
Efficiency (cooling)	5.2	2.56	1.34		

Table 6. Exogenous variables of residential equipment.

Type	Air Conditioner	Heat Pump Water Heater	Water Heater
Unit construction cost [USD/kW]	590	1360	43.6
Lifetime [year]	15	15	15
Efficiency (heating)	4.8	4.1	0.95
Efficiency (cooling)	5.3		

Table 7. Exogenous variables of battery storage.

Type	Li-Ion
Unit construction cost [USD/kW]	1320
Lifetime [year]	15
Cycle efficiency [%]	80
Usage rate [%]	90
Electric storage capacity [kWh/kW]	6

In contrast, for the industrial sector demand, only electricity demand was used in this model, because the general daily load curve for heat demand was unknown. The load pattern of electricity demand in the industrial sector was obtained by subtracting the electricity demand of the residential and commercial sectors from the area-wide electricity demand obtained from the literature [41], which was assigned to each node based on the energy consumption statistics of the industrial sector in each prefecture. The total demand for each sector is shown in Table 8.

Table 8. Energy demand in each sector.

	Commercial Sector				Residential Sector	Industry Sector
	Hotel	Hospital	Office	Store		
Electricity demand [TWh/year]	12.3	7.2	38.8	21	54.3	110.7
Cooling demand [TWh/year]	6.8	4.2	34.9	14.7	24.3	
Heating demand [TWh/year]	3.9	1.6	5.4	4	60.2	
Hot water demand [TWh/year]	7.7	2.5	0	0	89.8	

2.2.4. Other Settings

The year of analysis for this model was selected as 2030. The model considered four types of seasons: seasonal peak, summer, winter, and middle-season; three types of weather: sunny, cloudy, and rainy; and two types of days: weekdays and holidays. The number of days for each season and each weather condition was set as shown in Table 9, based on data from the Tokyo District Meteorological observatory [42]. The time period was set to 24 h/d. Fuel prices were set as shown in Table 10 with reference to the data from the World Energy Outlook [43].

Table 9. Number of days experiencing sunny, cloudy, and rainy weather under different season categories.

Weather [Days]	Sunny	Cloudy	Rainy
Seasonal peak	3	0	0
Summer (weekday)	32	22	27
Summer (holiday)	15	10	13
Winter (weekday)	54	8	19
Winter (holiday)	27	4	9
Middle (weekday)	44	15	25
Middle (holiday)	20	7	11

Table 10. Exogenous variables of fuel cost.

Type	Cost
Crude oil [USD/barrel]	88
Natural gas [USD/MMBtu]	9.7
Steam coal [USD/t]	86
Nuclear [USD/MWh]	18

As this model uses representative days for each season, and because it is difficult to set up a power generation curve for wind power, only PV was used as a renewable energy source. The total amount of PV installed in the model was adopted from the existing literature [44]. The amount of PV installed at each node was set as shown in Figure 6, with reference to the amount certified by the end of September 2018 under the feed-in tariff program [45].
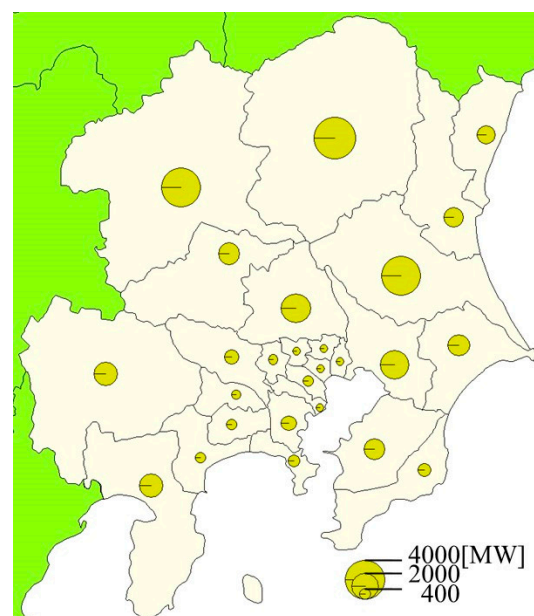

Figure 6. Amount of photovoltaic power generation capacity at each node.

The upper limit of CO_2 emissions was set at 84 Mt-CO_2/y based on Equation (7), accounting for the 46% reduction in CO_2 emissions by 2030, as indicated in the Sixth Strategic Energy Plan.

$$\sum_i \sum_j \sum_s \sum_t X_{i,j,s,t} \cdot eunit_j \cdot days_s + \sum_m \sum_s \sum_t Make_{m,s,t} \cdot gunit \cdot days_s \leq CO2_{upper} \quad (7)$$

CO_2 emissions for 2013 were set to 156 Mt-CO_2/y based on the amount of electricity generated (238.5 TWh) and city gas sold (14.0 Gm^3, excluding industrial use) per year in the National Capital Region in 2013, assuming that the CO_2 emission factor for all power sources was 0.521 kg-CO_2/kWh and that for city gas was 2.29 kg-CO_2/m^3.

2.2.5. Sensitivity Analysis

In recent years, the development of SOFC-CHP has been progressing steadily [46], and market introduction has been advancing, albeit gradually [47]. The most significant challenge for practical application is cost, and policy support for introduction is being provided through subsidies [48]. In this study, calculations were performed using the SOFC-CHP installed cost (Table 4) as the base value and decreasing the installed cost by up to 70%. From the results, the number and location of SOFC-CHP installation, power source configuration, and CO_2 emissions were confirmed.

3. Results and Discussion

The simulation results indicate that drastic cost reductions are necessary for the diffusion of SOFC-CHP. On the other hand, the results also indicate that the diffusion of SOFC-CHP can reduce the amount of power generation and CO_2 emissions in an economically reasonable manner. As the simulation results showed that SOFC installation starts when the reference cost decreased by more than 30%, cases below 20% were omitted.

3.1. Amount of SOFC-CHP Installation

The amount of SOFC-CHP and SGEN installed in each case is shown in Figure 7. First, SOFC-CHP is introduced in the residential sector when the installed cost attains a value 30% lower than the reference. When the installation cost decreases by 50%, SOFC-CHP is introduced in hotels and hospitals, where heat demand accounts for a relatively large share of total demand. In contrast, offices and stores, where heat demand is relatively small, SOFC-CHP introduction was not observed; SGEN is introduced when the installation cost falls by 70%.
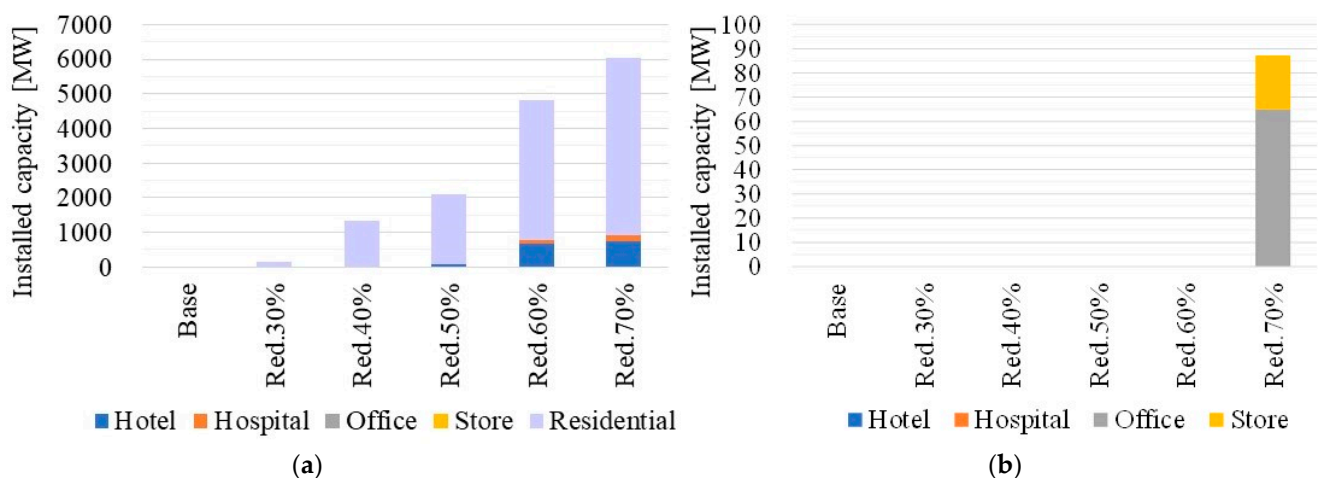

Figure 7. Installed capacity of (**a**) SOFC-CHP and (**b**) SGEN in each case. Red.% refers to the percentage reduction in installation costs.

Diffusion was defined in this study as the scenario in which SOFC-CHP is installed in 50% of the 26 demand nodes (13 nodes). To achieve this target, a 40% reduction in the installed costs in the residential sector, 60% reduction in the installed costs in hotels, and 70% reduction in the installed costs in hospitals would be required. Thus, radical cost reductions are required for SOFC-CHP diffusion into offices and stores.

One reason for the lack of SOFC-CHP installation in offices and stores is the lack of demand for hot water, as shown in Table 8 [34]. Considering the 60% installation cost reduction as an example, the residential sector, where SOFC-CHP is installed, possesses a large hot water demand, and the total SOFC-CHP waste heat for the entire residential sector is 20.3 TWh/y, of which 20.2 TWh/y is expected to be redirected for hot water demand. Similarly, for hotels and hospitals, where hot water demand is high, SOFC-CHP waste heat was observed to be 2.7 TWh/y for hotels and 0.45 TWh/y for hospitals, all of which are used for hot water demand. From this perspective, the presence of hot water demand significantly contributes to SOFC-CHP waste heat utilization. The results of this simulation are consistent with those arrived at by Sumitomo et al. [40]: they showed that for consumers with a large hot-water demand, economic feasibility can be achieved even with high SOFC-CHP installation costs; however, for consumers with low hot-water demand, economic feasibility cannot be achieved unless the SOFC-CHP installation costs are significantly reduced. In addition, as the electricity demand of offices and stores is approximately zero at night, the following obstacles would be experienced: a large difference in electricity demand between daytime and nighttime, and the restriction of the continuous operation of SOFC-CHP at a minimum load factor of 50% or more.

3.2. Location of SOFC-CHP Installation

It was found that geographical characteristics affect SOFC-CHP deployment. As an example of geographical characteristics, Figures 8–10 show the amount of SOFC-CHP installed at each demand node for representative cases of the residential, hotel, and hospital sectors. It can be observed that the installation of SOFC-CHP progresses from urban centers and spreads to suburban areas. This can be explained by comparing the annual average of shadow prices for electricity and city gas demand. Figure 11 shows the annual average of shadow prices for electricity and city gas at each demand node for the base case and the 70% reduction case. The difference in the figure represents the difference between the shadow price of electricity and that of city gas. In locations where the shadow price difference is large, the reduction in total system cost by reducing the supply of electricity and increasing the supply of gas is large. Therefore, SOFC-CHP is being deployed in urban centers, where the difference in shadow prices is larger, to help alleviate transmission congestion. For node 15, which possesses the largest shadow price difference, the shadow price of electricity in the base case was 0.199 USD/kWh, whereas when the installed cost of SOFC-CHP attains a value 70% lower than the base value, it was 0.188 USD/kWh. The electricity shadow price of node 15 would decrease by 9.4% with the installation of SOFC-CHP. The average shadow price of electricity for all nodes decreased by 7.6% from 0.188 USD/kWh (base case) to 0.174 USD/kWh (70% reduction case).

3.3. Power Source Configuration

The total power plant capacity and annual power generation in each case are shown in Figures 12 and 13. As shown in Figure 12, the installation of SOFC-CHP discourages the construction of new GTCC. When the installed cost of SOFC-CHP decreases by 60% from the base case, no new GTCC gets built. When the installed cost of SOFC-CHP decreased by 70%, the total capacity increased, because the installed capacity of SOFC-CHP is greater than the newly installed capacity GTCC in the base case. This indicates that a 70% reduction in the installed cost of SOFC-CHP renders the SOFC-CHP operation more economical than for the existing GTCC to generate power, resulting in the installation of more SOFC-CHPs than the required new power plant capacity.
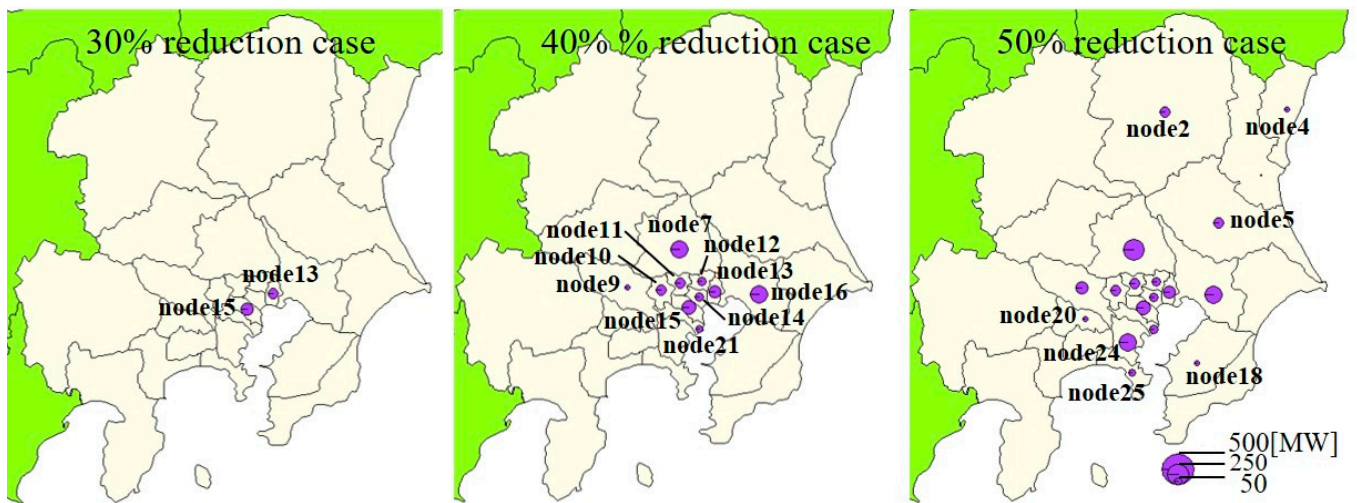
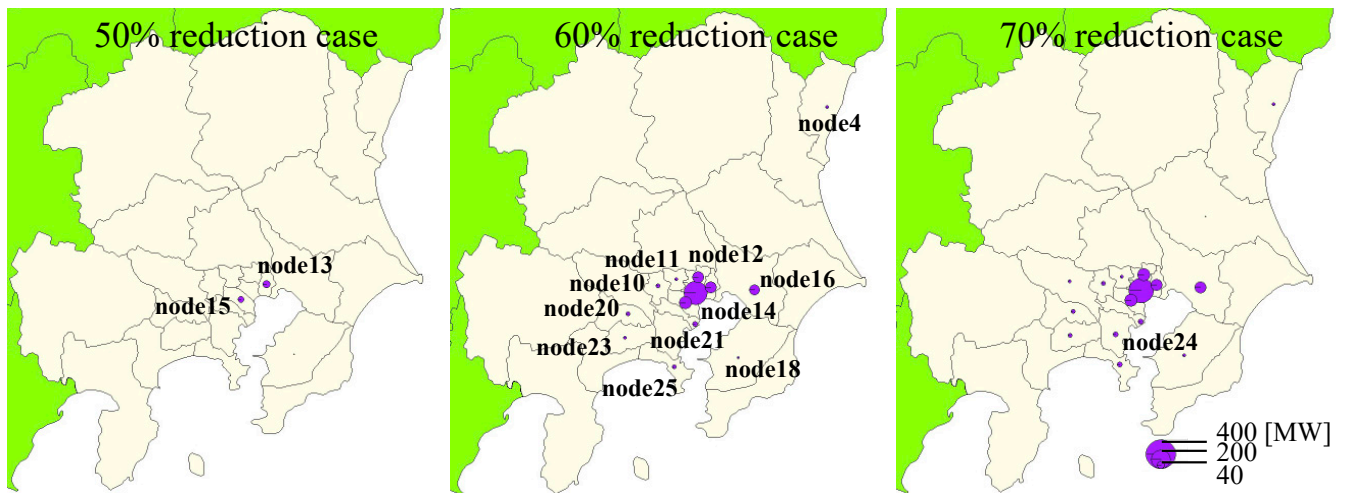**Figure 8.** State of SOFC installation area for the residential sector.

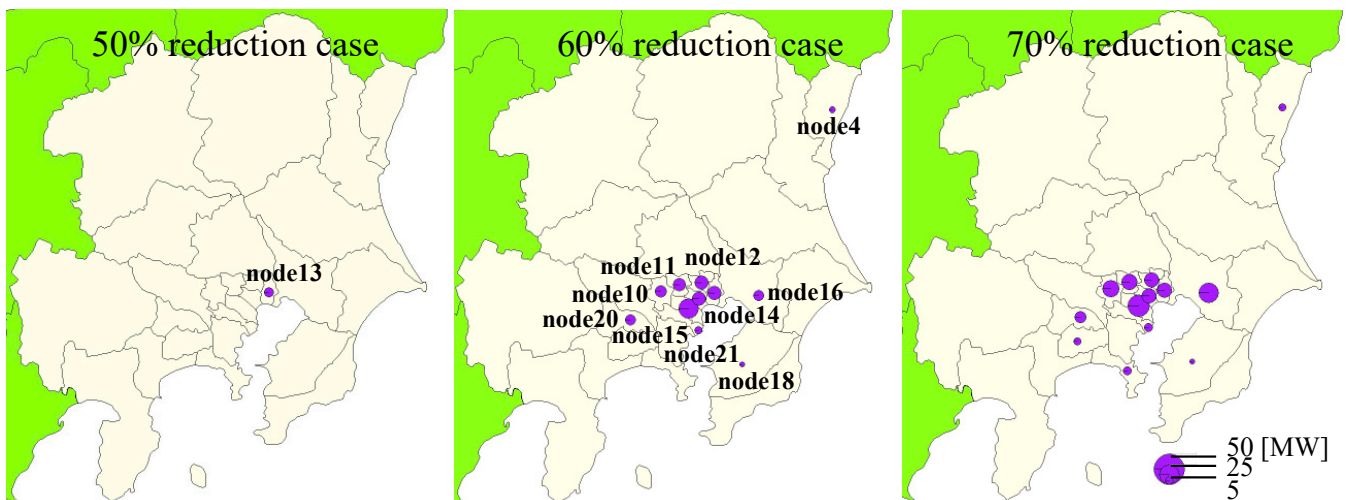**Figure 9.** State of SOFC installation area for the hotel sector.

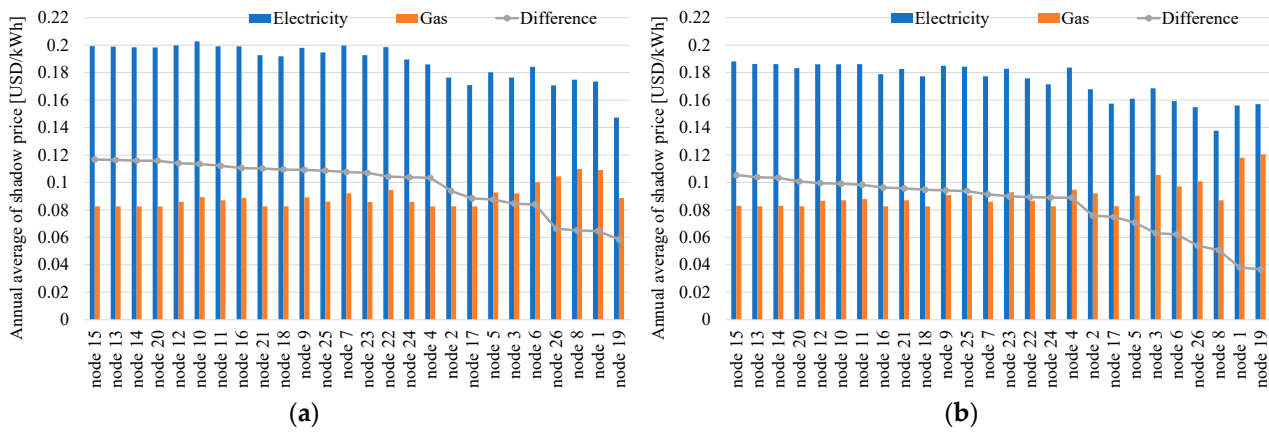**Figure 10.** State of SOFC installation area for the hospital sector.

Figure 11. Shadow prices of electricity and city gas at each demand node. (**a**) Base case; (**b**) 70% reduction case.
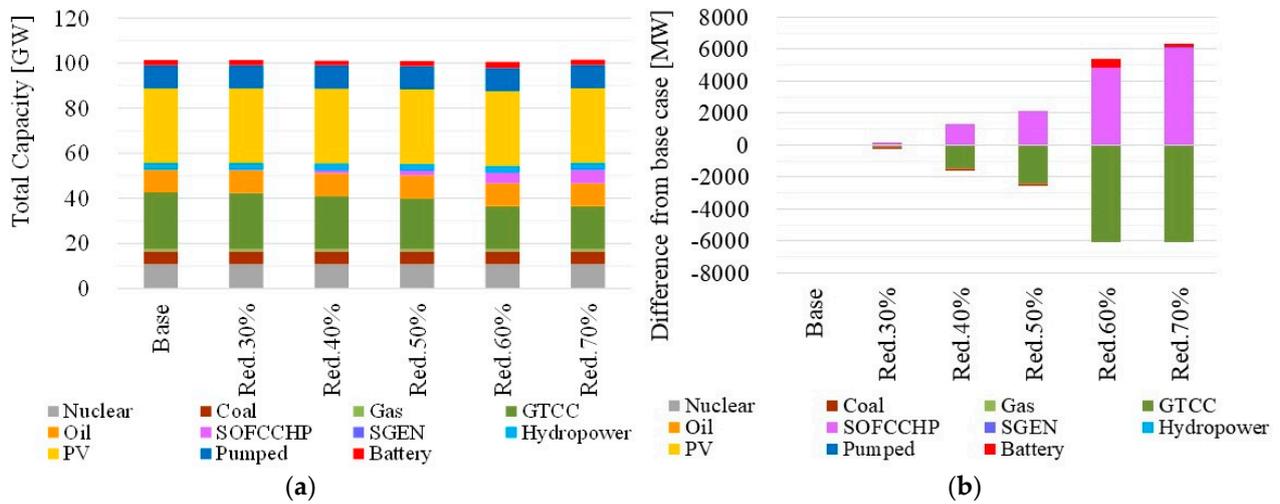

Figure 12. (**a**) Total power plant capacity in each case and (**b**) difference from base case. PV—photovoltaic power generation.
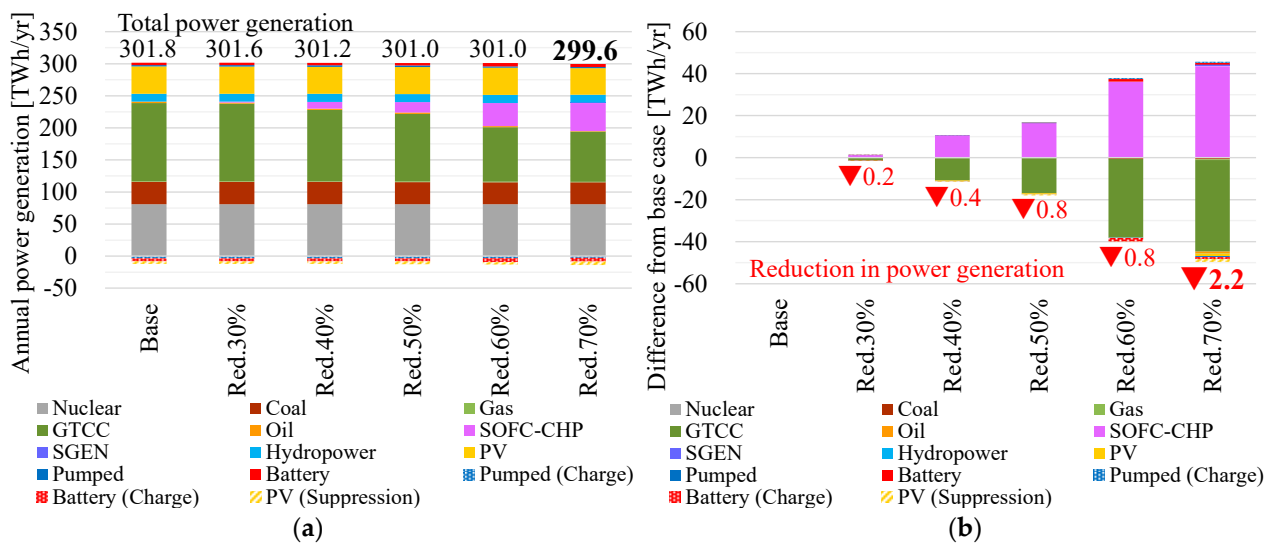

Figure 13. (**a**) Annual power generation in each case and (**b**) difference from base case.

As for power generation, Figure 13 shows that power generation from SOFC-CHP will first curtail power generation from GTCC, which was scheduled to be newly built. As the amount of SOFC-CHP installed increases, the amount of coal-, oil-, and gas-fired power generation at existing power plants will decrease. Although SOFC-CHP will continue to generate power at a minimum load factor of 50%, the introduction of SOFC-CHP will not significantly increase the output curtailment of solar power generation, the amount of pumped hydro power, or battery storage charge/discharge. It is expected to exert a marginal impact on the power supply composition. On the other hand, the introduction of SOFC-CHP decreases the amount of transmission and distribution losses, resulting in a decrease in total power generation. In the case where the installed cost of SOFC-CHP is 60% lower than the base case, total electricity production becomes 0.8 TWh/y lower than that in the base case, and in the case where the installed cost is 70% lower, the total electricity production was observed to be 2.2 TWh/y lower than that in the base case.

3.4. Carbon Dioxide Emission

The CO_2 emissions for each case are shown in Figure 14. The CO_2 reduction exceeded 46% in the case where SOFC-CHP is installed. This indicates that CO_2 emission reductions can be achieved in an economically feasible pathway without the CO_2 emission constraints, and that the diffusion of SOFC-CHP is crucial for CO_2 reductions. CO_2 emissions were observed to be further reduced by 2.5 Mt-CO_2 for 60% lower SOFC installation cost with respect to the base case and by 3.1 Mt-CO_2 for 70% lower costs than in the base case.
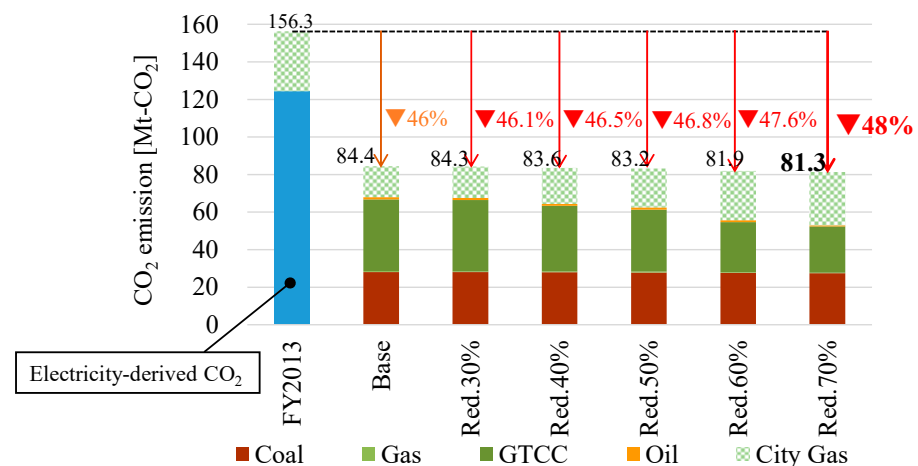

Figure 14. Carbon dioxide emission under different cases of installation cost reductions. FY2013—Fiscal Year 2013. The orange triangle indicates a 46% reduction; red triangles indicate an over 46% reduction.

3.5. Limitations of the Proposed Model

This study does not account for the wind power generation, because the simulation was calculated using representative days. Wind power together with PV is expected to contribute significantly to the future decarbonization of society and will be introduced in large quantities. Therefore, the introduction of wind power will exert an impact on the introduction of SOFC-CHP. Furthermore, in this study, each demand within a node is considered to be a single demand, and the amount of equipment installed was set to be linear, because a linear programming method was used; however, this differs from the actual situation in that the equipment was installed on a per-equipment basis for each customer's building. Nevertheless, although this study does not cover CHP in the industrial sector, the potential for introducing CHP in this sector is substantial, and further reductions in energy consumption and CO_2 emissions can be expected with the introduction of SOFC-CHP.

4. Conclusions

The novelty of this study is the development of an evaluation model that can simulate optimized facility configurations and operations with respect to supply and demand. The proposed model is unique, as it divides the target region into 26 demand nodes, each connected by 53 transmission lines and 34 gas pipelines, to account for the geographical characteristics, including the impact of energy transportation infrastructure. The evaluation model comprised three major components: a power grid sub-model, city gas grid sub-model, and consumer facilities sub-model. Each model was coupled by the supply and demand of electricity and city gas; by setting the final energy demand as electricity and heat demand, the model could optimize the facility configuration and operation based on the supply and demand. The following conclusions were obtained regarding the amount and location of SOFC-CHP installation, power source configuration, and CO_2 emissions:

1. Hot water demand as a percentage of demand was identified as a significant contributing factor for the introduction of SOFC-CHP. The simulation showed that the introduction of SOFC-CHP started with the residential sector, which exhibits the largest share of hot-water demand, followed by the hotel and hospital sectors. On the other hand, it was found to be difficult to introduce SOFC-CHP to offices and stores, where there is no demand for hot water supply. For SOFC-CHP to be spread over a larger area, installation cost in the residential sector ought to be reduced to 3870 USD/kW (40% lower than the base value). On the other hand, for the commercial sector, a significant cost reduction was required to spread SOFC-CHP compared to the residential sector: 1820 USD/kW for hotels (60% reduction from the base value), 1365 USD/kW for hospitals (70% reduction from the base value), and even greater reductions for offices and stores.

2. The introduction of SOFC-CHP was additionally dependent on geographical features; the introduction was observed to proceed from areas with large shadow price differences between electricity and city gas, thus alleviating transmission congestion. The study found that the average power shadow price of all demand nodes decreased by 7.6% when approximately 6 GW of SOFC-CHP was installed.

3. As SOFC-CHP was installed as a substitute for GTCC, even if SOFC-CHP became widely used, its impact on the amount of PV output suppression and battery storage recharge/discharge would be marginal. On the other hand, the diffusion of SOFC-CHP decreased the amount of transmission and distribution losses, resulting in a decrease in the total power generation. In this estimation, the amount of electricity generated decreased by 2.2 TWh/y when about 6 GW of SOFC-CHP was diffused.

4. The diffusion of SOFC-CHP will reduce CO_2 emissions in an economically feasible pathway. According to this estimation, if about 6 GW of SOFC-CHP was deployed, an additional reduction of 3.1 Mt-CO_2 emissions would be possible.

In future studies, it is necessary to consider wind power generation, as the spread of wind power generation facilities will expand, given the current trends in society. Therefore, the period under analysis must be modified to cover the entire year, because the simulation on a representative day cannot consider the variability of wind power generation. As this model was formulated as a linear programming model, it could not consider the startup and shutdown of power generation facilities. Therefore, this model ought to be modified to accommodate a mixed-integer programming model, in which the startup and shutdown plans are discrete variables. In addition, as this model does not consider the industrial sector, which possesses a large heat demand, the model ought to be additionally modified to consider the heat demand of the industrial sector in terms of verifying the effects of the diffusion of CHP. In the future, the authors intend to build a new evaluation model that accounts for these shortcomings and conduct more advanced verification of the effectiveness and optimal placement of SOFC-CHP and distributed generation.

Nomenclature

AD	Matrix components to calculate load flow
AF	Matrix components to calculate load flow
AG	Matrix components to calculate city gas flow
AP	Matrix components to calculate city gas flow
CO2upper	Upper limit of CO_2 emissions (84 Mt-CO_2)
days	Total days in a seasonal category (day)
De	Total electricity demand (kW)
DFIX	Amortization cost of consumer equipment
Dg	Total city gas demand (kW)
dloss	Distribution loss (2.5%)
EFIX	Amortization cost of power plants
EFUEL	Fuel cost of power plants
eunit	CO_2 emission intensity of power plants
F	Load flow of transmission lines
GFIX	Amortization cost of terminals and pipelines
GFUEL	City gas cost
gunit	CO_2 emission intensity of city gas
i	Index for power plant nodes (1 . . . 12)
j	Index for power plant types (1 . . . 7)
k	Index for transmission lines (1 . . . 53)
l	Index for demand nodes (1 . . . 26)
loss	Transmission loss (2.5%)
m	Index for terminal nodes (1 . . . 4)
Make	City gas terminal output (kW)
minLF	minimum load factor of SOFC (50%)
n	Index for pipelines (1 . . . 34)
p	Index for demand types (1 . . . 5)
PF	City gas flow of pipelines
s	Index for seasonal categories (1 . . . 19)
shonai	Power plant consumption rate (%)
SOFC	Installed CHP capacity of SOFC (kW)
SOFCop	Power output of SOFC-CHP (kW)
SGEN	Installed generator capacity of SOFC (kW)
SGENop	Power output of SOFC generator (kW)
St	Electricity for pumping (kW)
t	Index for time slots of a day (1 . . . 24)
TC	Total annual system cost (Objective function)
TFIX	Amortization cost of transmission and distribution equipment
X	Power output (kW)
Yall	Power plant capacity (kW)
zg	Maximum operation rate of power plants (%)
ze	Required reserve margin for power grids (5%)

References

1. United Nations Climate Change Conference (COP26) at the Scottish Event Campus Glasgow. 2021. Available online: https://ukcop26.org/cop26-goals/ (accessed on 13 October 2022).
2. Ministry of Economy, Trade and Industry. 6th Strategic Energy Plan. October 2021. Available online: https://www.meti.go.jp/english/press/2021/1022_002.html (accessed on 13 October 2022).
3. Ministry of Economy, Trade and Industry. Action Plan of the Green Growth Strategy for 2050 Carbon Neutral. December 2020. Available online: https://www.meti.go.jp/english/press/2020/1225_001.html (accessed on 13 October 2022).
4. United States Department of Energy. Combined Heat and Power Deployment Program Overview. 26 May 2021. Available online: https://betterbuildingssolutioncenter.energy.gov/resources/combined-heat-and-power-deployment-program-overview (accessed on 13 October 2022).
5. European Steel Association. Prioritising the Use of High-Efficiency Cogeneration by Industrial Operators to Reach 2030 Climate Goals. Available online: https://www.eurofer.eu/assets/publications/position-papers/prioritising-the-use-of-high-efficiency-cogeneration-by-industrial-operators-to-reach-2030-climate-goalsnew-publication-page/FINAL_Industrial-CHP-operators_2-03-22.pdf (accessed on 13 October 2022).
6. Li, X.; Wu, X.; Gui, D.; Hua, Y.; Guo, P. Power system planning based on CSP-CHP system to integrate variable renewable energy. *Energy* **2021**, *232*, 121064. [CrossRef]
7. Ahn, H.; Miller, W.; Sheaffer, P.; Tutterow, V.; Rapp, V. Opportunities for installed combined heat and power (CHP) to increase grid flexibility in the U.S. *Energy Policy* **2021**, *157*, 112485. [CrossRef]
8. Narayanan, M.; Mengedoht, G.; Commerell, W. Evaluation of SOFC-CHP's ability to integrate thermal and electrical energy system decentrally in a single-family house with model predictive controller. *Sustain. Energy Technol. Assess.* **2021**, *48*, 101643. [CrossRef]
9. Arinami, Y.; Sakaguchi, J.; Nakabayashi, S. Study on primary energy reduction effect by installing home-use fuel cell cogeneration system. *J. Environ. Eng. (Trans. AIJ)* **2019**, *84*, 687–697. (In Japanese) [CrossRef]
10. Yuasa, K.; Yata, M.; Niino, S.; Park, S. Evaluation on SOFC-CGS installation with consideration to electricity and hot water demand variation. *J. Environ. Eng. (Trans. AIJ)* **2015**, *80*, 543–550. (In Japanese) [CrossRef]
11. Aoki, T.; Shimoda, Y. Evaluation of residential fuel cell as the alternative to thermal power plants. *JSER* **2021**, *42*, 305–314. (In Japanese)
12. Nielsen, E.R.; Prag, C.B.; Bachmann, T.M.; Carnicelli, F.; Boyd, E.; Walker, I.; Ruf, L.; Stephens, A. Status on demonstration of fuel cell based micro-CHP units in Europe. *Fuel Cells* **2019**, *19*, 340–345. [CrossRef]
13. Palomba, V.; Ferraro, M.; Frazzica, A.; Vasta, S.; Sergi, F.; Antonucci, V. Experimental and numerical analysis of a SOFC-CHP system with adsorption and hybrid chillers for telecommunication applications. *Appl. Energy* **2018**, *216*, 620–633. [CrossRef]
14. Jing, R.; Wang, M.; Wang, W.; Brandon, N.; Li, N.; Chen, J.; Zhao, Y. Economic and environmental multi-optimal design and dispatch of solid oxide fuel cell based CCHP system. *Energy Convers. Manag.* **2017**, *154*, 365–379. [CrossRef]
15. Alns, A.; Sleiti, A.K. Combined heat and power system based on Solid Oxide Fuel Cells for low energy commercial buildings in Qatar. *Sustain. Energy Technol. Assess.* **2021**, *48*, 101615. [CrossRef]
16. Oshiro, K.; Masui, T. Analysis of long-term mitigation scenarios in Japan using multi-regional end-use model. *JSER* **2014**, *41*, 31–39. (In Japanese) [CrossRef]
17. Nagata, T.; Sano, F.; Akimoto, K. Analyses on the contribution of natural gas in the world and Japan as medium- and long-term global warming countermeasures. *JSER* **2020**, *41*, 196–208. (In Japanese) [CrossRef]
18. Sugiyama, T.; Komiyama, R.; Fujii, Y. Optimal power generation mix model considering nationwide high-voltage power grid in Japan for the analysis of large-scale integration of PV and wind power generation. *IEEJ Trans. Power Energy* **2016**, *136*, 864–875. (In Japanese) [CrossRef]
19. Johanna, B.; Lisa, G.; Fredrik, N.; Filip, J. A multiple system level modeling approach to coupled energy markets: Incentives for combined heat and power generation at the plant, city and regional energy system levels. *Energy* **2022**, *254*, 124337. [CrossRef]
20. Novoa, L.; Neal, R.; Samuelsen, S.; Brouwer, J. Fuel cell transmission integrated grid energy resources to support generation-constrained power systems. *Appl. Energy* **2020**, *276*, 115485. [CrossRef]
21. Shaffer, B.; Tarroja, B.; Samuelsen, S. Dispatch of fuel cells as Transmission Integrated Grid Energy Resources to support renewables and reduce emissions. *Appl. Energy* **2015**, *148*, 178–186. [CrossRef]
22. Abdullah, M.A.; Muttaqi, K.M.; Agalgaonkar, A.P. Sustainable energy system design with distributed renewable resources considering economic, environmental and uncertainty aspects. *Renew. Energy* **2015**, *78*, 165–172. [CrossRef]
23. Mike, B.N.; Sasa, Z.D.; Ignacio, H.G. Reliability Enhancement in Power Networks under Uncertainty from Distributed Energy Resources. *Energies* **2019**, *12*, 531. [CrossRef]
24. Takuma, T.; Hirohisa, A.; Kotaro, K.; Masayoshi, I. Assessment of utilization of combined heat and power systems to provide grid flexibility alongside variable renewable energy systems. *Energy* **2021**, *214*, 118951. [CrossRef]
25. Mathiesen, B.V.; Lund, H.; Karlsson, K. 100% Renewable energy systems, climate mitigation and economic growth. *Appl. Energy* **2011**, *88*, 488–501. [CrossRef]
26. Lund, H.; Möller, B.; Mathiesen, B.V.; Dyrelund, A. The role of district heating in future renewable energy systems. *Energy* **2010**, *35*, 1381–1390. [CrossRef]

27. Ministry of Economy, Trade and Industry. The Strategic Road Map for Hydrogen and Fuel Cells. March 2019. Available online: https://www.meti.go.jp/english/press/2019/0918_001.html (accessed on 13 October 2022).

28. Tokyo Electric Power Company. Information on System Empty Capacity. Available online: https://www.tepco.co.jp/pg/consignment/system/pdf_new/akiyouryou_kikan.pdf (accessed on 13 October 2022). (In Japanese).

29. Ministry of Economy, Trade and Industry. Report to the Subcommittee on Long-Term Energy Supply and Demand Outlook on the Verification of Power Generation Costs. May 2015. Available online: https://www.enecho.meti.go.jp/committee/council/basic_policy_subcommittee/mitoshi/cost_wg/006/pdf/006_05.pdf (accessed on 13 October 2022). (In Japanese)

30. *Gas Business Handbook 2021*; The Japan Gas Association: Tokyo, Japan, 2022. (In Japanese)

31. Ministry of Economy, Trade and Industry. Creating an Environment for Expanding Wholesale Trading Options. July 2014. Available online: https://www.meti.go.jp/shingikai/enecho/kihon_seisaku/gas_system/pdf/011_03_00.pdf (accessed on 13 October 2022). (In Japanese)

32. Tokyo Gas. Completion of the Construction of the Central Trunkline Phase II. Available online: https://www.tokyo-gas.co.jp/Press/20100507-01.html (accessed on 13 October 2022). (In Japanese).

33. The Society of Heating, Air-Conditioning and Sanitary Engineers of Japan. *Planning, Design and Operation for City Gas Cogeneration*; The Society of Heating, Air-Conditioning and Sanitary Engineers of Japan: Tokyo, Japan, 1999. (In Japanese)

34. The Society of Heating, Air-Conditioning and Sanitary Engineers of Japan. *Planning, Design and Operation for City Gas Cogeneration*; The Society of Heating, Air-Conditioning and Sanitary Engineers of Japan: Tokyo, Japan, 2015. (In Japanese)

35. Agency for Natural Resources and Energy. Energy Consumption Statistics by Prefecture. Available online: https://www.enecho.meti.go.jp/statistics/energy_consumption/ec002/results.html#headline2 (accessed on 13 October 2022). (In Japanese)

36. *National Hotel All Guides*; Yama-kei Publishers Co., Ltd.: Tokyo, Japan, 2002. (In Japanese)

37. Health Policy Study Group of the Ministry of Health, Labour and Welfare (Ed.) *Hospital Handbook*; Igaku-Shoin Ltd.: Tokyo, Japan, 2000. (In Japanese)

38. *Large-Scale Retail Stores in Japan*; Toyo Keizai Inc.: Tokyo, Japan, 2002; Volume 5723, p. 6. (In Japanese)

39. Ministry of Internal Affairs and Communications, Establishment and Enterprise Census. Available online: https://www.e-stat.go.jp/en/stat-search/files?page=1&toukei=00200551&tstat=000001008978&result_page=1 (accessed on 13 October 2022).

40. Sumitomo, S.; Akisawa, A.; Ikegami, T.; Nakayama, M. Installation effects of solid oxide fuel cell cogeneration for commercial buildings. *J. Jpn. Inst. Energy* **2019**, *98*, 149–156. (In Japanese) [CrossRef]

41. Tokyo Electric Power Company. Download Past Electricity Demand Data. Available online: https://www.tepco.co.jp/en/forecast/html/download-e.html (accessed on 13 October 2022).

42. Tokyo District Meteorological Observatory. Daily Weather Appearance Rate in Tokyo (Statistical Period 1981–2010). Available online: http://www.data.jma.go.jp/tokyo/shosai/bocho/tenki/link.html (accessed on 13 October 2022).

43. International Energy Agency. World Energy Outlook 2019. Available online: https://www.iea.org/reports/world-energy-outlook-2019 (accessed on 13 October 2022).

44. Ministry of the Environment. *Report of the Examination of Feasibility of Dissemination of Distributed Energy Such as Renewable Energy in 2050*; Ministry of the Environment: Tokyo, Japan, 2014. (In Japanese)

45. Website for Publication of Feed-In Tariff Information- the Official Web Site of Agency for Natural Resources and Energy. Available online: https://www.fit-portal.go.jp/servlet/servlet.FileDownload?file=0150K000006oQgY (accessed on 13 October 2022). (In Japanese)

46. BOSCH. How Stationary Fuel Cells Are Revolutionizing the Power Supply. Available online: https://www.bosch.com/stories/sofc-system/ (accessed on 13 October 2022).

47. The Japan Gas Association. Development Status and Future Prospects for Residential and Commercial Use of SOFC Systems. Available online: http://www.gas.or.jp/en/newsletter/images/22/dl/pdf01.pdf (accessed on 13 October 2022).

48. Tokyo Metropolitan Center for Climate Change Actions. Project to Promote the Formation of Smart Energy Areas Using Hydrogen (Business and Industrial Sector). Available online: https://www.tokyo-co2down.jp/subsidy/hydrogen_smart_biz (accessed on 13 October 2022). (In Japanese).